Volcanic-hosted epithermal systems in northwest Turkey

F. Pirajno
Geological Survey of Western Australia, 100 Plain Street, East Perth, W.A. 6004, Australia

Accepted 24 October 1994

Oligocene to Pliocene calc-alkaline volcanic rocks in the Biga peninsula, northwestern Turkey, host a number of precious and base metal hydrothermal mineral deposits. The nature of the hydrothermal alteration, mineralization, and the geochemical character of these deposits indicate that they are of the high-sulphur epithermal type. In terms of their geotectonic setting, the volcanics and contained epithermal deposits can be compared either to the Basin and Range province of the U.S.A., or to an Andean-type continental margin. Field observations, drill core, petrological, and geochemical studies are used to construct an ore deposit model and define an idealized pattern of alteration.

Oligoseense tot Plioseense kalk-alkaliese vulkaniese gesteentes in die Biga skiereiland, noordwes Turkye, bevat 'n aantal edel- en onedelmetaal hidrotermiese delfstofafsettings. Die aard van die hidrotermiese verandering, mineralisasie, en die geochemiese aard van hierdie afsettings dui aan dat dit van hoëswael epitermiese tipe is. In terme van die geotektoniese ligging, kan die vulkaniese gesteentes en die epitermiese afsettings wat in hulle voorkom vergelyk word met óf die 'Basin and Range' provinsie van die V.S.A., óf met die Andes-tipe kontinentale rand. Veldwaarnemings, kernbeskrywings, petrologiese, en geochemiese studies word gebruik om 'n ertsafsettingmodel te konstrueer en 'n geïdealiseerde patroon van verandering te definieer.

Introduction

Areas of the Biga peninsula, in northwestern Anatolia, Turkey, are underlain by volcanic and intrusive rocks ranging in age from the Eocene to the Pliocene. These rocks have a calc-alkaline to alkaline chemistry and are tectonically linked to episodes of subduction and extension, related to the northward movement of the African-Arabian plate.

In this environment a number of hydrothermal mineral occurrences and deposits are present. The origin of most, if not all, can be related to the waning phases of calc-alkaline

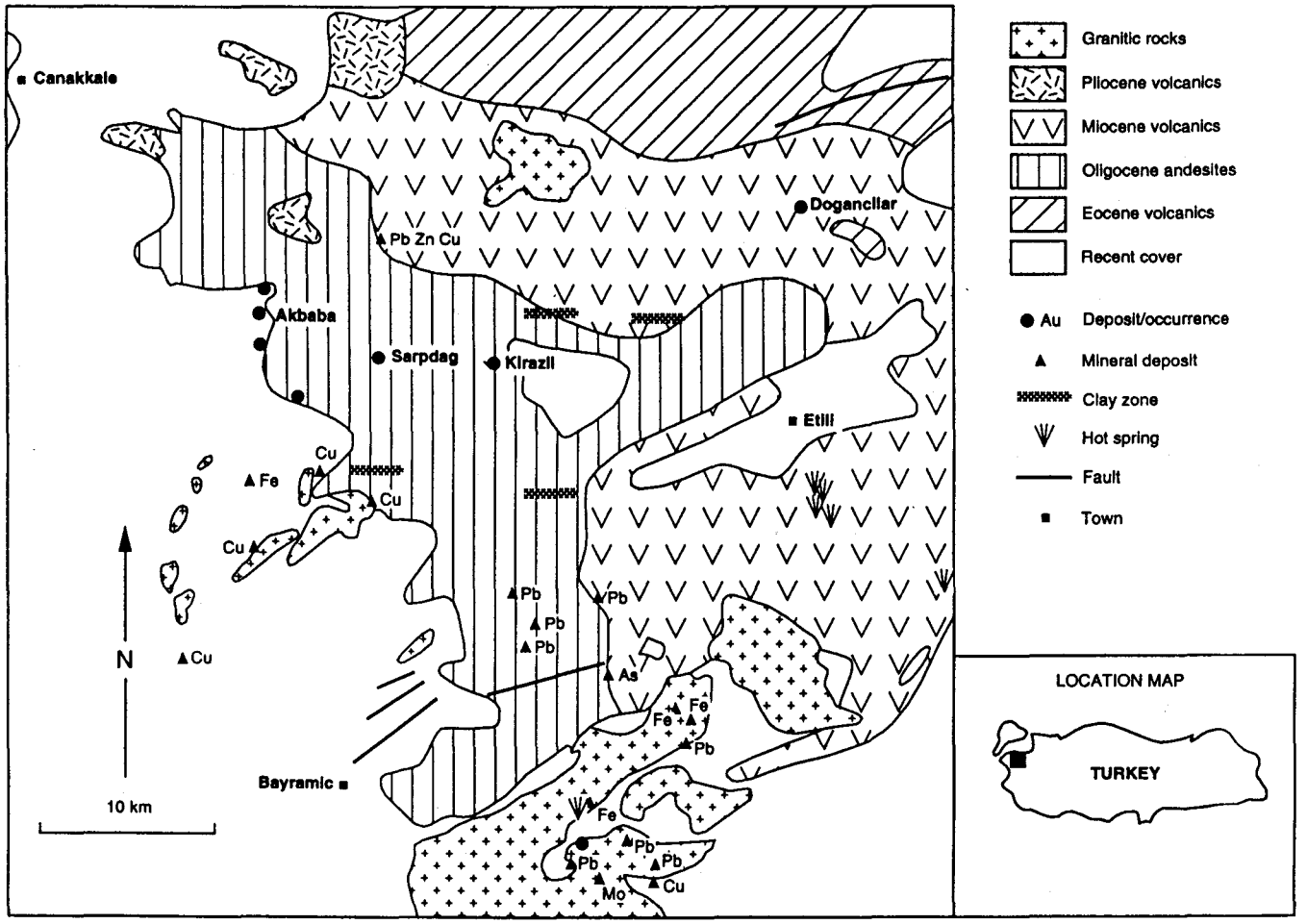

Figure 1 Simplified geological map of the Canakkale Volcanic Field (CVF) showing distribution of known mineral deposits and location of prospects visited.

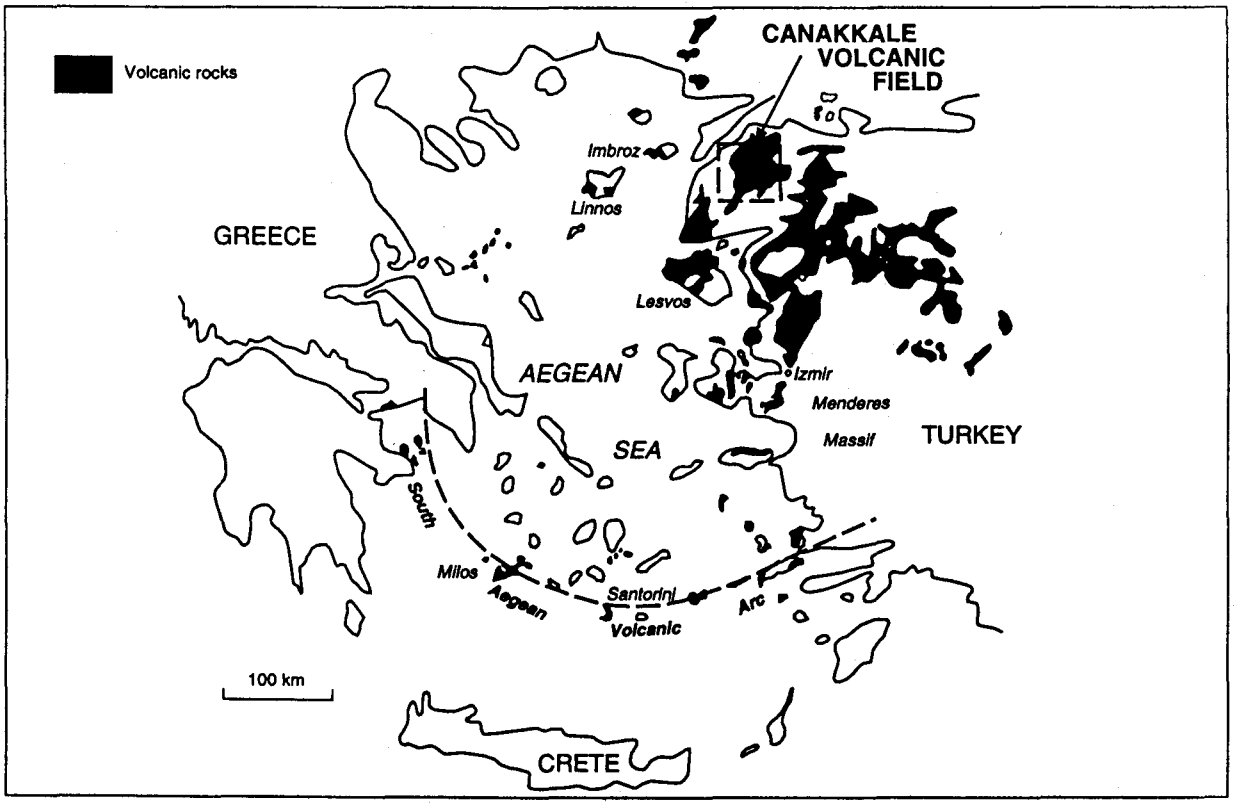

Figure 2 Distribution of Tertiary and Quaternary volcanic rocks in western Turkey and in the Aegean. Modified from Borsi *et al.*, (1973).

magmatism in the Biga region. Two areas in particular — Kirazli and Dogancilar (Figure 1) — contain precious metal deposits which are under current investigation by mining concerns.

Although many of the deposits in the Biga peninsula have been exploited since ancient times, little or nothing is known about their nature and origin. In the present work, the results of field observations, core logging, petrological, and limited lithogeochemical studies are reported, and a tentative ore deposit model is presented.

The Canakkale Volcanic Field (CVF) is an informal name given to an area underlain by volcanic rocks and allied intrusives in a portion of the Biga peninsula. The position of the CVF in western Turkey is illustrated in Figure 2. Information on the CVF is derived from an integration of the present work with available English-language literature on the volcanics of western Turkey (Seyitoglu & Scott, 1992; Yilmaz, 1989; 1990; Ercan, 1990; Borsi *et al.*, 1973; Innocenti & Mazzuoli, 1973). Yilmaz (1989) gives an exhaustive list of the work carried out on the volcanic rocks of western Turkey (Figure 2), all of which, apart from those mentioned above, are in Turkish. Yilmaz, also lamented the lack of detailed geological mapping, and the lack of knowledge of the volcanic stratigraphy and emphasized that little is known of volcanic episodes and their time-space relationship in the regional context.

The volcanic rocks of western Turkey, to which the CVF belongs, range in age from Oligocene to Pliocene and occupy areas in the Biga peninsula, along the coast between Izmir and Canakkale and extend approximately 200 km inland. To the west, the volcanics continue into some of the Greek islands (e.g., Lesvos, Linnos, and Imbroz), with lesser areas of exposure in European Turkey (Figure 2).

Geochemically, the volcanics of Western Turkey (and the Biga peninsula) can be subdivided into two associations: calc-alkaline and alkaline (Yilmaz, 1989; 1990). Temporally the calc-alkaline volcanism tends to precede the alkaline phase.

Rock types of the CVF include basalt, andesite, dacite, rhyodacite, rhyolite, alkali basalt, trachybasalt, trachyte, and trachyandesite. They occur as lavas, domes, and extensive pyroclastic deposits (e.g., ignimbrites, airfalls, and debris flows).

Geotectonic framework

The details of the tectonic history of this part of Turkey are poorly known and the various models proposed for the broader Anatolian–Eastern Mediterranean region (e.g., Robertson & Dixon, 1985; Sengör & Yilmaz, 1981; Sengör, 1992), do not adequately explain the observed magmatic and structural features of the CVF in particular, and western Turkey in general. Nevertheless, a schematic view of the tectonic and magmatic evolution of the area between the Menderes massif (Figure 2) in the south, and the Biga peninsula in the north, can be deduced from the literature cited above.

The earliest CVF volcanism began in the Late Cretaceous to Palaeocene as a result of the north-dipping subduction of the leading edge of the Neo-Tethys oceanic crust beneath the Pontide arc. In the Palaeocene, the northern Tethys had closed, but north-dipping subduction of a segment of Neo-Tethys branch, beneath the microcontinental fragment of Sakarya, was well developed. It is likely that a substantial portion of the CVF was formed during this geotectonic phase.

The strong north–south compression, along the entire Turkish orogen, continued between the Eocene and the Early Miocene with crustal thickening and possible delamination of subcontinental lithosphere, followed by partial melting of the lower crust to produce anatectic granitic melts in western Anatolia and in the Aegean islands. The north–south compression also resulted in the uplift of the Anatolides and the subsequent development of the Menderes metamorphic complex. Volcanism continued with the production of calc-alkaline volcanics in western Anatolia and the Aegean islands.

From the Pliocene to the Present a regime of north–south extension occurred in western Anatolia, owing to the 'westward' escape of the Anatolian plate. This westward escape is thought to be the result of the northward push exerted by the Arabian plate in the southeast, which forced this part of Turkey to move westwards into the more ductile eastern Mediterranean oceanic floor (Sengör & Yilmaz, 1981).

In conclusion, it is believed that the change of tectonic regime from compressional to extensional, resulted in a change from a dominantly calc-alkaline volcanism to a dominantly alkaline volcanism (Yilmaz, 1989; 1990). The precious metal mineralization discussed in this paper is linked to the former event. This view has, however, been challenged by Seyitoglu & Scott (1992) who, on the basis of trace element geochemistry, relate the change in the nature of the volcanism, not to the regional tectonic regimes (compressional–extensional), but to a thinned, extended lithosphere and increasing contributions from the asthenosphere.

Seyitoglu & Scott (1992) envisage two distinct magma sources to account for the calc-alkaline and alkaline volcano–plutonic products. Calc-alkaline magmatism was related to the beginning of extensional tectonism between the Late Oligocene and the Early Miocene, and the source is considered to have been a lithospheric mantle metasomatized by earlier subduction. Later, during more advanced stages of extension between the Late Miocene and the Pleistocene, the dominantly alkaline magmatism was sourced from the asthenosphere. It is interesting to note that Seyitoglu & Scott (1992) compare the northeastern Aegean and western Anatolia region to the Basin and Range province in the U.S.A., whereas other authors (e.g., Okay *et al.*, 1994) compare it to an Andean-type continental margin.

Regional volcanic geology

The plutonic and volcanic rocks in the Biga peninsula and the rest of western Anatolia have been subdivided into three distinct suites (Yilmaz, 1990), namely: 1) granitic suite; 2) andesitic suite; and 3) basaltic suite. The granitic and andesitic suites belong to a calc-alkaline to shoshonitic series, whereas rocks of the basaltic suite are part of an alkaline series. The volcanic rocks rest on a basement of metamorphic rocks (mainly schist) of Permo-Triassic age.

The granitic suite includes granitic (quartz–monzonite) stocks, radial and concentric dykes, rhyolite lava domes, flows, and associated ignimbrites, ranging in age from 35 to 23 Ma (Zimmerman *et al.*, 1989; Yilmaz, 1989). The spatial and temporal relationship of the extrusive rhyolitic rocks with the granitic rocks are reported to be well displayed in the Ezine–Ayvacik area (southern Biga peninsula) (Yilmaz, 1989). The rhyolitic rocks commonly exhibit perlitic textures, whilst eutaxitic textures are well displayed in the ignimbrites. Initial Sr^{87}/Sr^{86} ratios range from 0.710 to 0.720 and they can be interpreted in terms of a continental crust signature (Yilmaz, 1990).

The andesitic suite is represented by andesite, latite, dacite, rhyodacite, and related pyroclastic sequences. These rocks occur as lava domes, blocky lava flows, flow breccias associated with ignimbrite sheets, airfall tuffs, volcaniclastic sediments, and debris flows. Yilmaz (1989) considers that the andesitic volcanics were erupted from strato-volcanoes. However, either because of erosion or lack of adequate aerial observations or both, volcanic edifices, or their remnants, have not been recognized in the area. The lavas of the andesitic suite are dark- to light-coloured and usually porphyritic, with phenocryst contents from 25 to 50% by volume. Plagioclase is usually well-zoned and is typically andesine with compositions ranging from An_{25} to An_{60}, but more commonly around An_{38-40}. Oscillatory zoning is characteristic. Pyroxene phenocrysts are represented by diopsidic augite and enstatite. The groundmass of the andesitic volcanics is characterized by plagioclase microlites, in places showing a trachytic texture, pyroxene granules, Fe oxides, and glass.

Ignimbrites are rhyodacitic in composition and are formed by broken crystals (crystal tuffs) and lithic blocks in a glassy eutaxitic matrix. The crystals are comprised of zoned oligoclase-andesine, biotite, sanidine, and quartz.

CIPW norms indicate that rocks of the andesitic suite are quartz and orthopyroxene normative. Geochemically rocks of the andesitic suite have large silica variations (58% in andesite to 73% in rhyolite). Total alkalies are also high, ranging from 5 to 8% and therefore they are K-rich calc-alkaline andesites. The andesitic volcanics are also enriched in LIL (large ion lithophile) elements, with Rb ranging from 100 to 250 ppm, Ba from 800 to 1250 ppm, and Sr from 230 to 700 ppm; but poor in HFS (high-field strength) elements such as Nb (9 to 18 ppm) and Zr (100–200 ppm). Ti is also low (0.7–0.8%). Initial Sr^{87}/Sr^{86} ratios range from 0.703 to 0.708 (Yilmaz, 1990).

Basaltic volcanism is of Pliocene to Quaternary age and therefore later than the granitic and andesitic suites, although in places there may be some overlap with the calc-alkaline rocks. Basalts were probably erupted from fissures or from a series of fault-controlled monogenetic vents. Phonolite and tephrite are fine-grained porphyritic rocks in which feldspathoid is an essential component. They contain nepheline, sanidine, and clinopyroxene. The olivine basalts are characterized by phenocrysts of labradorite, olivine, and Ti-rich augite. The trachybasaltic series is characterized by hornblende as a common mafic phenocryst with plagioclase less calcic than in the olivine basalts.

The basaltic suite has an alkaline chemistry and is represented by a range of basaltic rocks. They comprise two subseries, with distinct geochemical and Sr isotopic signatures. One is a mildly alkaline, low-Ti series (1.2–1.4% TiO_2; Sr_i 0.703–0.705) including trachybasalt, hawaiite, and mugearite. The other is a strongly alkaline, high-Ti series (approximately 2% TiO_2; Sr_i of 0.702–0.703) characterized by olivine basalt, phonolite, and tephrite.

Epithermal gold deposits

Introduction

The CVF is endowed with numerous occurrences and deposits of precious and base metal mineralization, most of which are spatially associated with extrusive and intrusive rocks. The distribution of these occurrences is illustrated in Figure 1. In this area, Pb appears to be the most common metal, followed by Cu, Au, Zn, Fe, and Mo. Quartz and barite are common gangue minerals. Hot springs and low pH, ambient-temperature, mineral springs also occur in the area testifying to ongoing hydrothermal activity.

East–northeast-trending lineaments are discernible on LANDSAT TM imagery. These trends may have exerted a structural control on the mineralization.

Hydrothermal alteration and silicification are widespread and affect all rock types to varying degrees. Silicification (chalcedony, opaline silica, and crystalline quartz) is particularly common and it can be seen to form sub-horizontal sheets, usually along hill tops. This silica is normally barren, but at a number of localities is associated with precious metal mineralization. The significance of this silica is discussed later. Apart from silicification, hydrothermal alteration styles include propylitic (epidote, chlorite, calcite, pyrite, gypsum, and ankerite) phyllic (sericite, pyrite, illite, and quartz), argillic (kaolinite, dickite, smectite, and illite), and advanced argillic (pyrophyllite and alunite). Hydrothermal breccias are present and appear to be spatially and perhaps, genetically, associated with Au mineralization.

Geological and geochemical data indicate that the gold prospects in the area belong to the category of volcanic-hosted high-sulphur epithermal type. They include hydrothermal veins (Akbaba), stockworks (Dogancilar), and a combination of stockworks, breccia, disseminated and replacement systems (Kirazli, Sarpdag) (Figure 1). The mineralized localities discussed in the present work are at Kirazli and Dogancilar.

Kirazli

The Kirazli prospect, is located approximately 1.5 km south of the village with the same name (Figure 1).

Exploration work led to the identification of two ore zones: a high-grade oxide ore zone and a low-grade sulphide ore zone. The high-grade oxide ore forms a sub-horizontal zone, approximately 200 m long x 100 m wide x 5 m thick. Data on ore reserves are proprietary, but grades range from 2 to 20 g/t Au.

The low-grade sulphide ore zone, considered as a possible underlying root or 'feeder', is approximately 200 m long x 30 m wide x 75 m thick. The precise geometry of the ore zones is not known, but they are thought to be irregular with barren patches between areas of Au-bearing material.

The mineralization is hosted in altered pyroclastic units of the andesitic series in the CVF.

Hydrothermal alteration and nature of the mineralization

Field observations, petrological, and mineralogical work have revealed a complex pattern of hydrothermal events. Silicification, brecciation, sericitic, argillic, and advanced argillic alteration have occurred, resulting in several stages of overprinting. Gold mineralization appears to be related to all of the above-mentioned events. In addition, weathering has caused intense oxidation and re-distribution of some of the mineral phases. There are no significant quartz veins at Kirazli.

In general, textural relationships indicate that a spatial and temporal pattern (possibly temperature-related) of quartz–sericite–pyrite (below 700 m a.s.l.) overprinted and followed upward (700 – 730 m a.s.l.) by a phase of hydrothermal brecciation with an assemblage of quartz–pyrophyllite–epidote and an assemblage of clay–barite–alunite–pyrite. The clay minerals are mainly kaolinite and dickite (XRD identification). The presence of pyrophyllite and epidote in the former suggests that this is a higher temperature assemblage (e.g., Meyer & Hemley, 1967; Henley & Ellis, 1983) compared to the latter. These assemblages are, in turn, followed towards the surface by a second influx of silica-saturated fluids, resulting in an upper zone of chalcedonic hydrothermal breccia. This phase probably broke through a pre-existing, brown to light grey, sub-horizontal silicified zone. This zone is of regional extent, forming prominent ridges or cliffs and can be shown to have been formed by the replacement of permeable pyroclastic units.

The spatial and temporal trend (possibly temperature-related), is reflected in the vertical distribution of the altera-

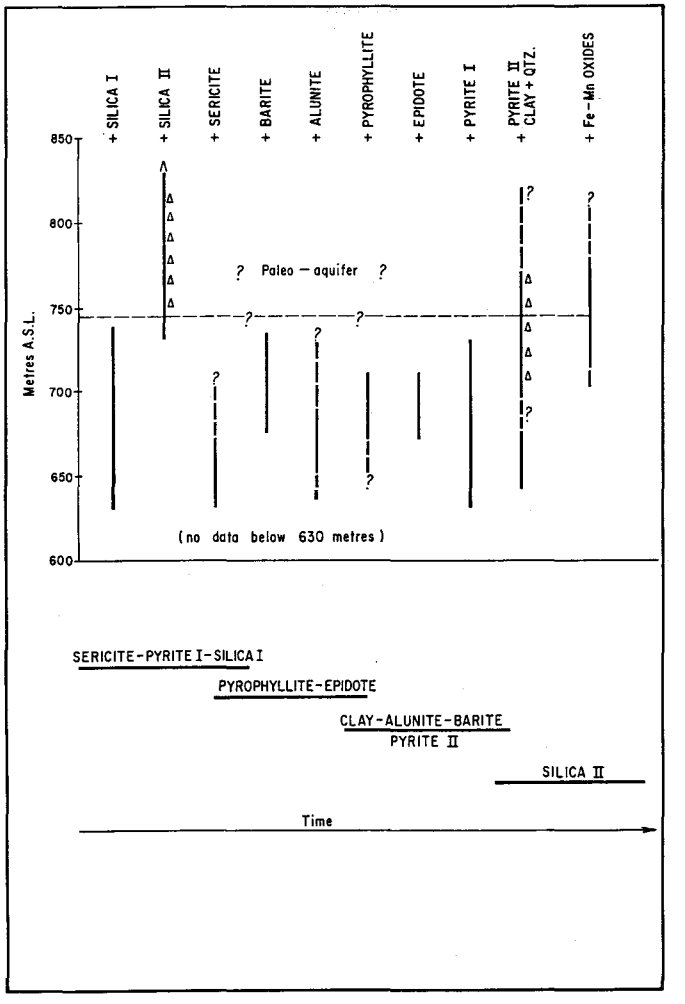

Figure 3 Tentative vertical distribution of alteration minerals and approximate paragenetic sequence at Kirazli.

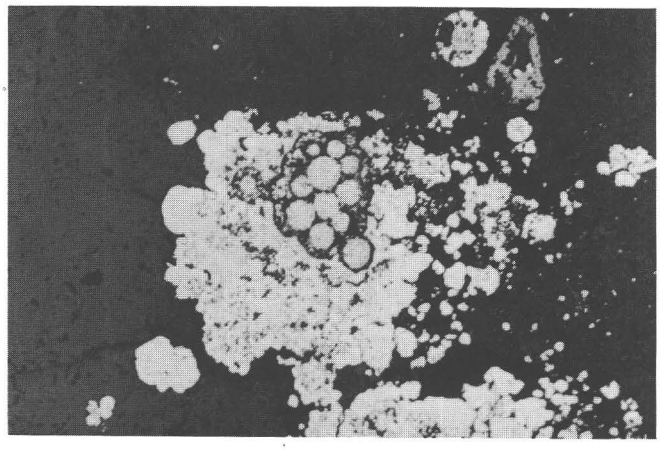

Figure 4 Reflected light photomicrographs of pyrite spheroids from Kirazli. Width of field of view is approximately 3 mm.

tion minerals shown in Figure 3, where a tentative paragenetic sequence is also given.

The sulphides are almost entirely represented by pyrite. Famatinite was identified in a mineralogical investigation carried out by Newmont Ltd. (D. Volkert, pers. comm., 1992), but not seen during the present study. At Kirazli pyrite occurs in two different modes, as disseminated grains and as veinlets. In addition, at least three morphological types or phases are recognized. The most common pyrite occurs as disseminated euhedral crystals or masses, normally associated with the quartz–sericite alteration assemblage. Pyrite veinlets fill microfractures and are associated with hydrothermal breccias and the clay–barite–alunite alteration assemblage. A third morphological type is represented by tiny spheroids (<0.1 to 0.25 mm in diameter), which occur isolated or as aggregates up to 1 mm in length (Figure 4). The spheroids consist of a round central nucleus, surrounded by a shell of radially arranged crystallites. Textural relationships indicate that the pyrite spheroids are late and overprint the euhedral pyrite.

Similar pyrite spheroids have been recorded in epithermal environments elsewhere (e.g., Drake Cu–Au field in New South Wales, Australia) (England & Oswald, 1993). It is interesting to note that the mineralogical investigations carried out by Newmont Ltd. revealed that 70% of the pyrite is of the first type (euhedral) and is As-rich and Au-poor. The pyrite spheroids are, by contrast, As-poor and Au-rich.

In summary it appears likely that late, lower-temperature solutions precipitated Au-rich pyrite in a high-sulphur hydrothermal system. The same hydrothermal system also produced the quartz–pyrophyllite alteration at lower levels, and hydrothermal breccias with advanced argillic, barite–alunite–clay alteration and pyrite veinlets alteration at higher levels. This event(s) overprinted an earlier one in which quartz–sericite–pyrite and silicification had occurred. Gold also occurs as free particles associated with Fe oxyhydroxides (goethite and limonite). The association of the gold with Fe oxyhydroxides suggests its dissolution from a primary site (e.g., pyrite spheroids) and reprecipitation in the weathering environment under conditions of low pH. Remobilization of gold from sulphides and its subsequent association with late Fe oxyhydroxides is a feature also found in the epithermal deposits of the Nansatsu district in Japan (Hedenquist *et al.*, 1994). In the oxidized zone Mn hydroxides, oxysilicates, and oxides (e.g., braunite and manganite) and leucoxene (an alteration product of titanite) are also present.

Dogancilar

This prospect is located approximately 3 km from the village of the same name, some 19 km east–northeast of the Kirazli-Sarpdag area (Figure 1).

The area affected by alteration–mineralization covers approximately 20 km^2 and is characterized by a prominent hill (Karadag, 749 m a.s.l.; Figure 5) formed by silicified pyroclastic units. In addition to extensive silicification, Au-bearing stockworks, barite and sulphide-bearing veins, and a site interpreted as a fossil fumarole, are present at Dogancilar.

Hydrothermal alteration and nature of the mineralization

Dominant structures in the area are east–west and west–northwest. Gold mineralization has been noted to be associated with Cu and Ba (barite) in the Bakirlik vein and stockwork zone, at elevations of 500 – 550 m a.s.l., where values of between 4 and 10 g/t Au and up to 2.8% Cu are recorded. The Bakirlik vein is hosted in hydrothermally altered andesitic volcanics. Alteration assemblages include quartz–sericite and illite–montmorillonite (XRD identification). Barite occurs as isolated crystals.

Near the top of the hill (Karadag; Figure 5) a west–northwest-trending structure contains significant Ag (120 ppm), As (10 000 ppm), and Pb (3840 ppm) at an elevation of approxi-

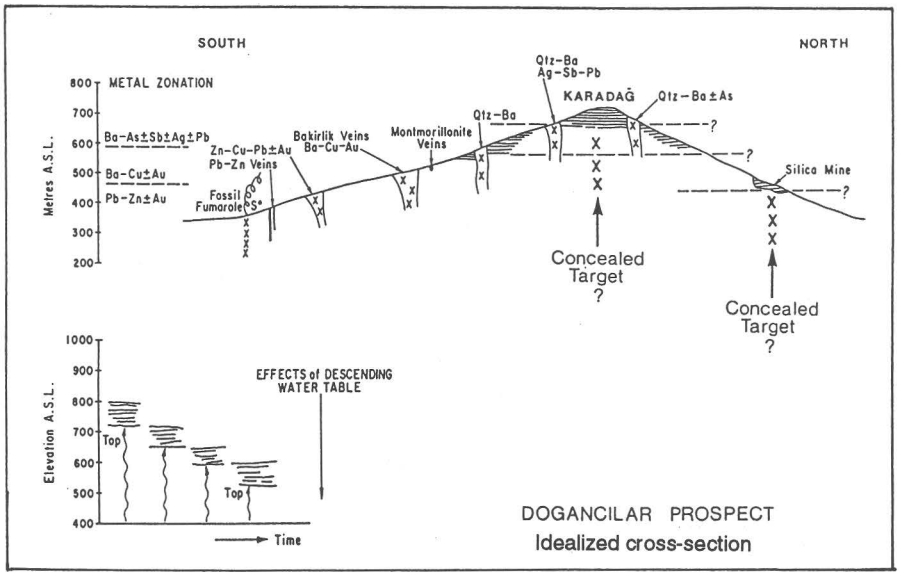

Figure 5 Schematic cross-section of Karadag hill - Dogancilar prospect - showing position of mineralized localities and inferred metal zoning. See text for details.

mately 720 m a.s.l. From the 550 m a.s.l. contour to the top of the hill there are outcrops of intensely silicified material. This silicification consists primarily of chalcedonic quartz with colloform textures. Brecciated zones are present and locally display hydraulic fracturing and/or fluidization textures. Silicification is gradational and ranges from stockwork veinlets in clay-altered volcanics to progressively more abundant silica veining until the entire rock mass is replaced by chalcedonic quartz, brecciated and healed by new influxes of silica. Barite is locally present and associated with at least one of the silica phases.

The 'Silica Mine' (Figure 5) is a locality approximately 1.5 km east of Karadag, where silica is mined for industrial uses. In this area total replacement of a pyroclastic unit has occurred. The replaced rock consists of a dense, fine, granular, quartz aggregate with very fine pyrite disseminations. Spring waters (ambient temperature) near this quarry are mineralized with Fe hydroxides and have pH values ranging from 4.5 to 3.5.

In the southeast of the area, at an elevation of approximately 390 m a.s.l., veins containing sphalerite and galena occur. Geochemical analyses of chip samples from these veins have returned values of 3% Pb and 7% Zn. The veins are less than 2 m wide and have an approximate east–west strike. The wallrocks are fractured and pervasively altered to an assemblage of quartz, kaolinitic clay, and pyrophyllite. Pyrophyllite selectively replaces phenocrysts and is in turn replaced by the kaolinite clay.

About 170 m south of these veins a structurally-controlled zone of pervasive alteration occurs. Here, pyroclastic rocks are hydraulically fractured, have thin quartz stockworks, and show pervasive clay + pyrite alteration. These altered rocks also exhibit encrustations of native sulphur. The alteration is characterized by halloysite and kaolinitic clays, locally with illite intergrowths, replacing groundmass and phenocrysts. Pyrite occurs as fine disseminations. This locality is interpreted as the site of ancient fumarolic activity.

A vertical zonation from Ba–As–Ag–Pb ± Sb in the upper levels, Ba–Cu–Au in the middle, to Pb–Zn ± Au in the lower levels is apparent from the current data (Figure 5).

Hydrothermal geochemistry

Trace and major element geochemical (Tables 1 and 2) were used in order to gain insights into the element associations and variations in the altered, mineralized, and unaltered rocks. A simple statistical approach (correlation coefficients and factor analyses) was used together with spidergram plots of values normalized to selected 'base lithologies'. However, because of the limited data, the results reported and discussed in this study must be taken with caution and can only be considered as an indication of generalized trends.

Element associations for Kirazli and Dogancilar, derived from correlation matrices and factor analyses, are shown in Tables 3 and 4 respectively.

Kirazli and Dogancilar share both similar and different geochemical features and this is readily evident from the element correlations and factor analyses presented in Tables 3 and 4. They have in common the association of the elements Pb, Sb, and As. Although this association does not necessarily imply a mineralogical expression, it is possible that the Pb, Sb, and As are hosted in sulphide or sulphosalt phases in the system. The plot of Figure 6 illustrates this association rather well.

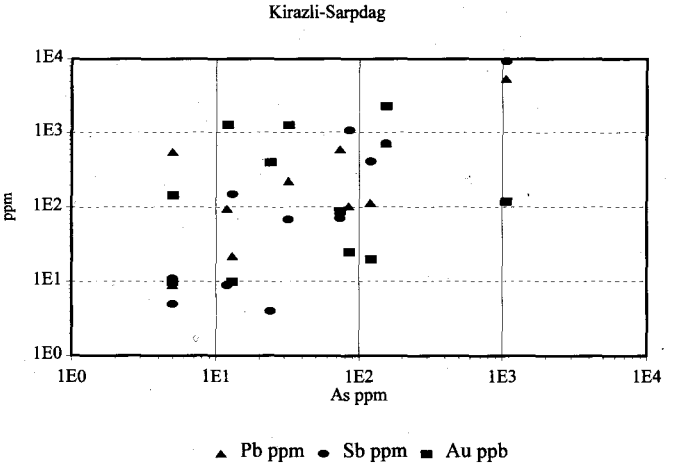

Figure 6 Binary plot of arsenic (As ppm) v. lead (Pb ppm), antimony (Sb ppm), and gold (Au ppb).

Gold, in terms of metal associations, on the other hand, shows remarkable differences between the two prospects. At Kirazli there is a positive correlation between Au, Hg, and Ba, whilst the opposite is observed at Dogancilar.

In both areas there is no correlation between Au and As. At Kirazli (Table 3) factors 1 and 2 are probably the result of discrete alteration–mineralization events. The role of trace elements, such as Nb and Y, is owed to hydrothermal alteration effects of wallrocks. Nb is normally associated with alkali metals (Na and K) whilst Y may reflect the presence of chlorite or other phyllosilicate minerals. Argillic and advanced argillic alteration tends to destroy K- and Na-bearing phases (e.g., feldspars, micas, and sericite), this would result in a decrease of the alkali metals together with Nb and an increase in Y.

At Dogancilar (Table 4) factor 1 appears to relate to a base metal mineralizing event. There is a negative correlation between Ba and Au and a weak positive correlation between Au and F. Factors 2 and 4 are possibly related to hydrothermal alteration, whereas factor 3 may reflect a phase of high level precious metal mineralization.

A series of plots (Figures 7A–C) reveal some very important differences between the unaltered volcanics and the altered–mineralized volcanics. Within the latter there are some differences which can be useful in discriminating the type of alteration.

Figure 7A shows a spidergram of Pb and Au normalized to an average andesite. The Pb–Au landscape appears flat in the unaltered rocks, but it becomes very rugged in the altered–mineralized material showing a sympathetic relationship between the two elements. The precise reason for this correlation is not known, but two mechanisms are possible. One is that Pb-bearing sulphosalts might be present, which in the weathering zone result in the residual concentration of Pb together with the chemical concentration of Au in a low pH environment. The second reason is that there is a distinct regional Pb (and Sb) provinciality in western Turkey. In fact,

Table 1 Selected trace element analyses of altered-mineralized and unaltered rocks

Sample	Zn	Cu	Mo	Nb	Zr	Y	Sr	Rb	Pb	As	Sb	Te	F	Ba	Ti	Hg ppb	Au ppb	Ag
REC-3	52	51	6	17	203	31	581	102	15	5	5	13	650	787	4538	10	20	1
REC-5	116	51	6	15	189	44	583	84	13	5	5	9	420	803	5415	10	10	1
REC-7	49	26	7	18	206	33	438	130	22	5	5	5	890	794	4556	10	10	1
REC-8	40	3	4	13	214	25	231	139	19	5	5	15	400	953	2384	10	10	1
REC-10B	76	34	7	10	73	28	258	31	5	5	5	7	560	323	6344	10	10	1
REC-14	52	12	2	9	98	18	346	90	14	5	5	6	430	694	2850	44	10	1
REC-15	54	12	3	8	114	19	478	71	12	5	5	10	640	608	3186	10	10	1
REC-18	75	30	3	9	68	24	271	17	5	5	5	6	310	173	4220	10	10	1
REC-21A	56	34	6	10	105	26	680	67	9	5	5	4	250	686	3148	10	10	1
REC-21B	58	21	3	10	103	20	258	83	9	5	5	4	670	681	3996	10	10	1
REC-22A	24	60	7	10	121	33	239	116	8	17	5	7	360	872	5532	10	10	1
REC-22B	27	125	3	12	134	16	256	79	56	17	5	4	590	813	5547	10	10	1
REC-23	75	33	2	22	187	27	52	89	5	22	5	6	590	464	8220	10	10	1
REC-24	44	3	5	19	186	33	99	207	24	10	5	4	460	473	1839	10	10	1
REC-25	78	112	6	8	49	21	749	43	5	22	5	4	50	270	4826	10	10	1
REC-26	76	28	3	14	215	40	395	90	13	5	5	16	710	561	5013	10	10	1
REC-28	331	30	4	24	190	34	34	105	16	23	5	4	660	460	8159	10	10	1
REC-29	83	9	4	7	100	21	620	56	5	5	5	8	370	796	3747	10	10	1
REC-30	93	34	3	9	100	18	215	24	12	22	5	4	470	326	3926	45	10	1
KIR-1	7	3	14	11	151	4	5	2	22	13	150	15	100	135	5985	360	10	1
KIR-2	7	26	4	11	115	8	652	2	600	74	72	19	720	241	3253	23000	90	10
KIR-3	8	705	7	19	140	4	816	2	710	154	713	14	260	3086	5279	17300	2285	33
KIR-4	8	14	2	4	64	2	2014	2	546	5	11	13	420	263	3779	1400	145	2
KIR-5	14	33	9	9	129	6	252	2	5374	1061	9373	10	660	333	4506	610	120	8
KIR-6	7	25	9	6	82	5	1424	2	397	24	4	5	1100	1239	4774	830	395	1
KIR-7	10	36	4	10	128	14	607	2	225	32	69	7	820	2386	5308	1100	1270	7
KIR-8	12	6	10	10	89	5	17	2	114	121	410	26	830	146	3638	66	20	1
KR8-7490	10	859	10	10	108	12	272	2	96	12	9	5	770	2400	4644	2070	1280	13
SARP-1	89	29	10	8	73	23	436	19	9	5	5	4	660	341	3924	10	10	1
SARP-2	4	12	11	7	89	2	265	2	103	85	1080	10	250	120	3620	10	25	1
DOG-1	10	3	2	2	18	8	19	18	7	37	11	5	1150	720	5863	10	195	1
DOG-2	4505	7308	17	9	25	16	22	20	1215	665	122	5	390	715	956	130	10	3
DOG-3	175	1826	5	15	198	33	60	192	40	31	16	5	670	1954	5015	10	10	1
DOG-8	67	23	9	9	85	7	42	2	32	9	85	5	140	4962	3501	120	10	1
DOG-14	10	6	5	14	235	7	5	2	5	5	5	7	120	146	7844	10	10	1
DOG-15	12	23	3	9	103	12	1532	2	29	38	5	17	65	2744	4946	10	65	1
DOG-16	42	3	9	8	116	14	76	7	102	5	5	11	550	1780	1808	10	10	1
DOG-18A	55	390	3	9	127	22	197	64	66	13	5	5	170	888	5547	10	10	1
DOG-18B	18	8	2	8	135	30	270	99	46	8	5	11	580	894	6458	76	10	1
DOG-18C	27	40	2	10	152	29	197	106	27	23	15	10	760	573	6370	10	10	1
D0G-19	222	418	5	13	130	24	36	3	27	257	20	5	210	212	7058	740	220	1
DOG-20	88	1253	4	10	156	30	77	21	9	5	5	5	730	2072	4192	10	10	1
DOG-21	387	1277	15	13	98	17	76	136	18	31	11	5	710	1448	2962	10	120	1
DOG-22	12	23	16	9	77	8	16	11	455	30	28	9	410	763	2342	10	10	1

Sample prefixes and numbers signify the following: REC 3, 5, 7, 8, 10B, 14,15, 18, 24, 28, 29 – unaltered andesitic volcanics; REC 21, 22 and 23 – variably altered volcanics; REC 25, 26 – tholeiitic basalt; REC 30 – dacite; KR 8-7490 and KIR 1 to 8 – altered host rocks and ore-bearing materials from Kirazli. SARP 1 and 2 – altered andesite and silica breccia respectively from Sarpdag. Samples from the Dogancilar prospect are: DOG 1, 2, 3 – altered wall rocks, DOG 8, 14 – massive silica; DOG 15, 16 – altered wallrock volcanics; DOG 18 – materials from fossil fumarole; DOG 19, 20, 21, 22 – altered and ore-bearing materials. All values are given in parts per million (ppm), unless otherwise stated (parts per billion, ppb). Analytical work was performed at ROCKLABS (Pretoria) by XRF on fusion discs

Table 2 Major element analyses of altered-mineralized and unaltered rocks

Sample	SiO_2	TiO_2	Al_2O_3	Fe_2O_3	MnO	MgO	CaO	Na_2O	K_2O	P_2O_5	H_2O^-	LOI	Total
REC-3	57.80	0.78	17.88	6.74	0.15	2.84	5.86	2.93	3.33	0.27	0.51	1.14	100.23
REC-5	56.98	0.81	18.31	6.29	0.09	2.70	6.14	2.89	3.00	0.25	0.51	1.60	99.57
REC-7	62.68	0.63	17.06	5.27	0.05	1.02	3.70	3.07	3.97	0.21	0.89	1.45	100.00
REC-8	69.23	0.31	14.94	1.57	0.07	0.46	1.81	3.44	4.10	0.07	0.68	3.06	99.74
REC-10B	45.26	0.98	16.57	11.22	0.25	3.92	6.77	2.95	0.99	0.17	0.56	9.70	99.34
REC-15	61.03	0.45	15.52	4.24	0.12	1.56	5.25	2.80	1.98	0.16	0.35	6.60	100.06
REC-24	71.35	0.27	14.34	1.91	0.04	0.38	0.68	2.88	5.55	0.07	0.75	1.73	99.95
REC-25	49.81	0.81	18.79	10.08	0.20	5.68	10.28	2.38	0.54	0.14	0.38	1.00	100.09
REC-26	61.08	0.72	17.52	4.98	0.10	1.82	5.13	3.55	2.36	0.22	0.65	1.94	100.07
REC-30	57.41	0.48	16.65	4.15	0.15	1.30	6.23	0.18	0.74	0.18	0.40	12.02	99.89
KIR6	60.60	0.61	24.57	4.07	0.01	0.10	0.11	0.02	0.02	0.29	0.10	9.48	99.98
KIR7	70.39	0.64	13.57	6.55	0.00	0.04	0.06	0.06	0.28	0.18	0.26	7.95	99.98
DOG-16	83.62	0.26	10.80	0.37	0.01	0.05	0.02	0.02	0.11	0.06	0.07	4.36	99.75

See caption of Table 1 for explanation of sample numbers. All values in weight per cent. Analytical work performed at ROCKLABS (Pretoria) by XRF on pressed discs

(A)

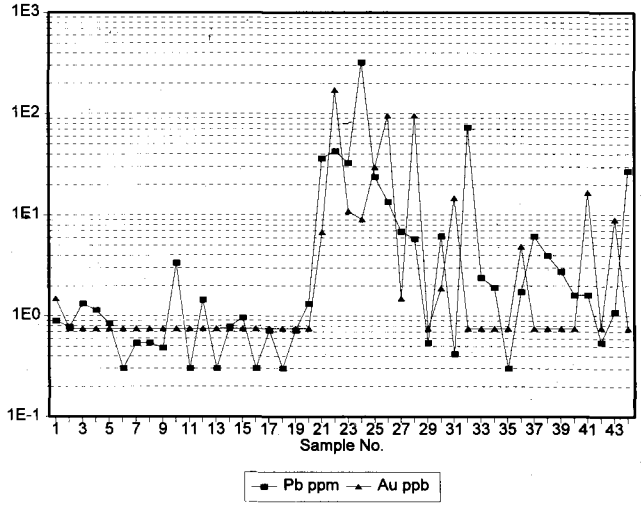

(B)

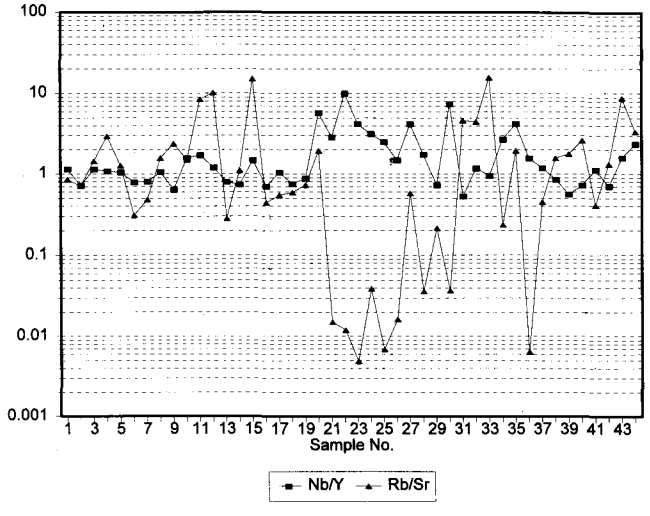

Pb and Sb appear to be the two commonest elements in most hydrothermal deposits.

A plot of Nb/Y and Rb/Sr, also normalized to an average andesite derived from the three analyses of CVF unaltered andesites is shown in Figure 7B. The plot indicates marked variations in these ratios from the unaltered on the left hand side (samples 1 to 19) to the altered–mineralized rocks (samples 20 to 44). The antipathetic behaviour of the Nb/Y and Rb/Sr ratios in the altered–mineralized rocks can be explained by alkali depletion (Rb) due to clay alteration concomitant with an increase in the Nb/Y ratio. The latter is controlled by

(C)

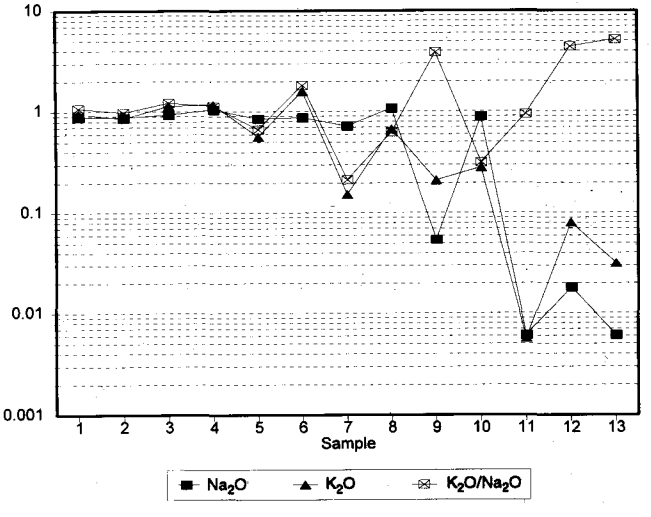

Figure 7 Lead (Pb ppm) – gold (Au ppb) (A), niobium/yttrium (Nb/Y) – rubidium/strontium (Rb/Sr) ratios (B), soda (Na_2O wt. %) – potash (K_2O wt. %) and soda/potash (Na_2O/K_2O) ratios (C), spidergrams normalized to an average unaltered andesite calculated from published analyses of volcanic rocks from Western Turkey (Borsi *et al.*, 1973; Innocenti & Mazzuoli, 1973) and analyses from present study.

Table 3 Factor analysis (performed using the STATGRAPHIC computer program) of chemical analyses from the Kirazli prospect

FACTOR 1	Ba–Cu–Au–Nb–Zr–Hg	Mineralization + alteration
FACTOR 2	Pb–As–Sb	Mineralization
FACTOR 3	Zn–Y–Rb	Hydrothermal alteration halo

Table 4 Factor analysis (performed using the STATGRAPHIC computer program) of chemical analyses from the Dogancilar prospect

FACTOR 1	Cu–Pb–Zn–As–Sb–Mo	Mineralization
FACTOR 2	Zr–Nb–Rb–Y	Hydrothermal alteration
FACTOR 3	F–Au–Rb–Hg	Alteration + mineralization
FACTOR 4	Ba–F–Sb–Rb	Hydrothermal alteration

the extent of phyllosilicate alteration (e.g., Y in chlorite or clay minerals) and the possible presence of Nb in alteration facies related to mineralization, as also suggested by the factor analyses. Figure 7C shows a spidergram of K_2O, Na_2O and their ratio, normalized to an average andesite. In this figure the unaltered rocks display a flat landscape. This landscape becomes increasingly rugged towards the right hand side (samples 6 to 10). The last three samples (11 to 13) represent ore-bearing samples from Kirazli. They display low alkalies, with samples 12 and 13 having high K_2O/Na_2O ratios. The interpretation in this case is that the samples affected by pervasive argillic alteration are strongly depleted in K and Na, owing to the destruction of feldspars and micas. The plot also suggests that there is little or no higher rank alteration (e.g., phyllic or potassic). If this were present it would register a strong enrichment in K_2O.

Discussion

The gold occurrences and deposits in the Canakkale district are hosted in calc-alkaline volcanic rocks of the CVF and at the interface between the metasedimentary basement and the overlying volcanics.

Study of outcrops and samples obtained from drilling to depths of approximately 200 m (e.g., Kirazli), indicate argillic, advanced argillic, sericitic, propylitic, and silica alteration styles surrounding and enclosing zones of stockworks, pyrite disseminations, and hydrothermal breccias. Alunite, barite, kaolinite, dickite, illite, pyrophyllite, montmorillonite, and abundant pyrite are some of the alteration minerals present. The alteration patterns and mineralogy of these deposits are consistent with a volcanic-related high-sulphur epithermal origin.

An important hydrothermal feature of regional extent in the CVF is the presence of sub-horizontal silicified zones, usually barren of mineralization and usually, but not always, forming topographic highs or cliffs. Field and petrological evidence indicates that these silicified zones are formed by varying degrees of replacement of pre-existing lithologies, generally high-permeability pyroclastics units, resulting in pervasive silicification. Chert, chalcedony, and opaline silica are the main phases of this silicification. In places, this silica is strongly leached and a cavernous or vuggy residue is left behind. This type of leaching by acid fluids is commonly observed in high-sulphur epithermal deposits (e.g., Hedenquist *et al.*, 1994).

Examination of core specimens from Kirazli suggests a vertical zonation, as illustrated in Figure 3. One of the main features of this zonation are that quartz, sericite, pyrite, epidote, alunite, and pyrophyllite all occur below 750 m a.s.l. and towards the upper levels they are all overprinted by a later phase of silica alteration. Textural evidence indicates that kaolinitic clays + alunite overprint an earlier phase of quartz + sericite + pyrite alteration. It is also important to note that this late phase of quartz–clay–pyrite alteration is accompanied by hydrothermal brecciation.

Apart from an association of gold with Fe hydroxides in the near surface weathering zones, the precise siting of gold is not known. It is possible, however, that some of the gold resides within the spheroidal pyrite, which is associated with the late phase of clay–quartz–pyrite alteration and hydrothermal breccias. Again, gold remobilization and its concentration in Fe oxyhydroxides is observed in several epithermal districts (Sillitoe *et al.*, 1990; Hedenquist *et al.*, 1994).

At Dogancilar there is field evidence that the regional silicification is very thick (approximately 250 m). There is also evidence that vertical alteration zoning, although reasonably well-defined for metals (typically lower levels Pb–Zn evolving upward into Cu–Ba–Au and Ba–Ag–Sb–As–Pb), is unclear in respect of alteration minerals. But at Dogancilar too, alteration minerals all occur below a certain level (approximately 600 m a.s.l.). The Dogancilar alteration–mineralization field covers a large area and the presence, in at least one place, of native sulphur associated with pervasive clay alteration and pyrite, suggests the presence of a fossil fumarolic field.

Tentative ore deposit model and conclusions

The data presented in this work are not sufficient to provide a well-constrained ore deposit model. Nevertheless, the prospects examined — Kirazli, Dogancilar, Akbaba, and Sarpdag — although spatially separated can be fitted into a unifying genetic working model. A number of important features must be considered in order to formulate a conceptual model that could reasonably well explain the observed characteristics. Some of these characteristics are listed below:

1) widespread regional silicification of permeable pyroclastic units;

2) the mineral prospects are characterized by disseminations, fine stockworks, and breccias, and except for Akbaba, there is a general lack of significant quartz veins;

3) argillic and advanced argillic alteration with disseminated pyrite, in places mineralized with gold and other metals;

4) presence of, locally Au-bearing, hydrothermal breccias;

5) common presence of barite and anomalous Pb;

6) presence of native sulphur and clay–pyrite alteration at Dogancilar at the same topographic level as Pb–Zn sulphide veins; and

7) low-pH mineral springs;

The regional sub-horizontal zones of silica replacement of pyroclastic units, probably represents a silica-saturated palaeoaquifer which formed the upper portions of a very

extensive hydrothermal system, powered by volcanic heat. This palaeoaquifer was pervasively silicified during ongoing hydrothermal activity. A similar situation is thought to have occurred in the Early–Middle Miocene, high-sulphur epithermal systems of northern Chile (Sillitoe, 1991).

The palaeoaquifer was topographically controlled and, as the area underwent rapid tectonic uplift, the aquifer progressively descended, so that now one can observe several levels of regional silicification. This is seen at Dogancilar, where pervasive tabular silicification occurs some 250 m below the

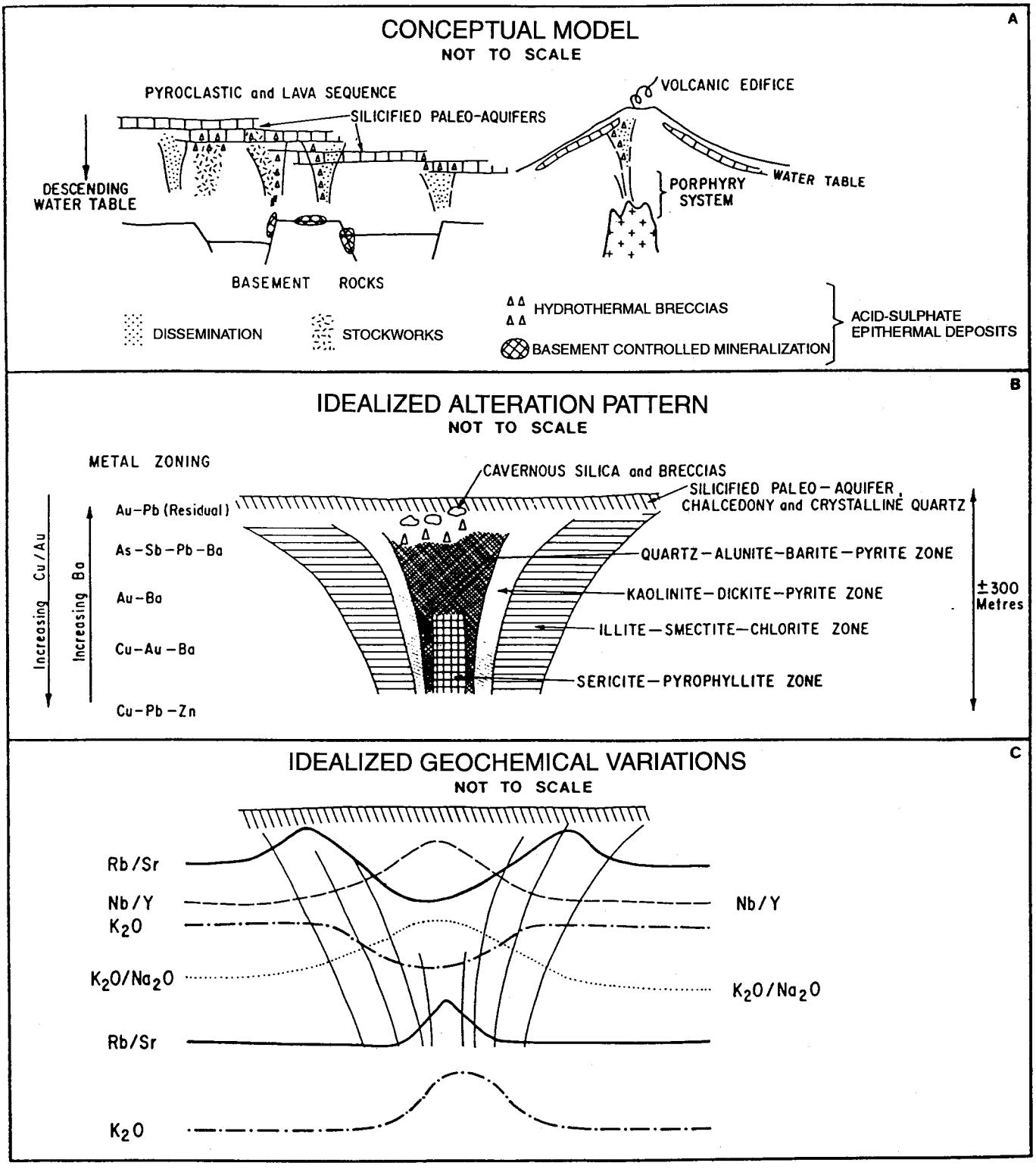

Figure 8 Ore deposit model (A): Kirazli–Sarpdag and Dogancilar would be located within the pyroclastic-lava sequence at left; the volcanic edifice and subjacent porphyry system depicted on the right are hypothetical. Idealized alteration pattern (not to scale) is shown in (B), whereas the geochemical variations that may be applicable to the model are given in (C). See text for details.

top of the hill (Karadag). The effects of a descending water table are illustrated in the inset of Figure 5.

The silicified aquifer, at various stages, acted as an impermeable barrier to continuously rising hydrothermal solutions. In a number of places the fluids broke through this barrier, whenever the fluid pressure exceeded the tensile strength of the overlying siliceous barrier. This resulted in extensive brecciation, locally accompanied by precipitation of gold. Fumarolic activity continued, even after erosion began dismantling the upper silicified palaeoaquifer levels and exposing the lower portions of the underlying epithermal deposits. This is shown at Dogancilar, where acid leached rocks, encrusted with native sulphur, occur alongside Pb–Zn-bearing veins. Low-pH mineral springs still issue at a number of places, between Kirazli and Dogancilar, testifying to this ongoing hydrothermal activity.

The proposed working model is shown in Figure 8A, together with schematic, qualitative, representations summarizing alteration patterns (Figure 8B) and geochemical trends, both in the vertical and horizontal sense (Figures 8B and C). In this model the epithermal deposits of the CVF were formed at the interface between basement rocks and the overlying volcanic cover, and in the highly permeable pyroclastics predominantly as stockworks and disseminations, owing to the weakly competent and porous nature of these rocks. Alteration ranged from argillic to advanced argillic in a predominantly acid-sulphate environment. Supergene Fe oxyhydroxides, derived from the oxidation of the abundant disseminated pyrite, commonly accompany the argillic zones and display enhanced gold values, probably due to chemical reconcentration of the metal under low pH, weathering conditions. The quartz–alunite–barite–pyrite grades downward into quartz–sericite–pyrophyllite and laterally to kaolinite–dickite–pyrite and illite–smectite to propylitically altered rocks (Figure 8B). Ledges of cavernous and porous silica, commonly seen at Kirazli for example, are indicative of extreme acid leaching, which left behind residual silica and hydrothermal breccias containing most of the gold mineralization. Barite is especially abundant at Dogancilar, where it increases upward and commonly lines open spaces in silicified and clay-altered rocks.

The sericite–pyrophyllite association is important because it may form haloes to bonanza-type zones. Its identification, together with key geochemical parameters (e.g., alkali ratios, Nb/Y, Rb/Sr, and Cu/Au ratios) can be of great importance in an attempt to identify possible underlying porphyry systems. It is also possible that high-sulphidization or acid-sulphate environments may directly overlie a porphyry system (e.g., Mitchell, 1992; Sillitoe, 1991).

The results of this work suggest that the CVF is a province of acid-sulphate epithermal-type precious metal mineralization (Heald *et al.*, 1987) associated with a subduction-related volcanic arc of calc-alkaline to alkaline affinity. Acid-sulphate epithermal environments are known to be spatially and genetically linked with porphyry systems at depth. Therefore, the mineral potential of the CVF is augmented by the possibility of porphyry (Cu–Au?) occurrences. However, our current knowledge of the volcanic geology of the CVF, its evolution, stratigraphy, and above all, the original volcanic landforms (e.g., strato-volcanoes, vent areas, calderas etc.) is rudimentary at best. Considerable more field work, detailed geochemical, and petrological studies are necessary to unravel the complexities of the region and to improve the chances of mineral discoveries.

Acknowledgments

I wish to express my gratitude to John Raubenheimer, Stan Hausmann, and Andy Jackson (GENMIN, South Africa), for providing the opportunity of working at this project. John Raubenheimer gave the permission to publish this paper.

I also extend my gratitude to Klaus Rellensmann, Director of Tüprag, Dave Bickford, Chief Geologist and geologists Dave Volkert, Gunter Herget, Thomas Gülden, Paul Kuhn, Ilhan Bettemir, Mevlüt Avsan, Stephen Maynard, and Yücel Oztas for their hospitality and for sharing their knowledge with me.

Constructive criticism from two reviewers have improved the manuscript. Andrew Goss, of the Department of Minerals and Energy of Western Australia, kindly provided the bromide prints of the figures.

References

Borsi, S., Ferrara, G., Innocenti, F. & Mazzuoli, R. (1973). Geochronology and petrology of Recent volcanics in the eastern Aegean Sea (West Anatolia and Lesvos island). *Bull. Volcanologique*, **36**, 473–496.

Bove, D., Rye, R.O. & Hon, K. (1988). Evolution of the Red Mountain alunite deposits, Lake City, Colorado. *Abstr. with Programs, Geol. Soc. Am.*, **20**, A353.

England, B.M. & Ostwald, J. (1993). Framboid-derived structures in some Tasman fold belt base-metal sulphide deposits, New South Wales, Australia. *Ore Geol. Rev.*, **7**, 381–412.

Ercan, T. (1990). Geology of the area between Balikesir and Bandirma, petrology and regional distribution of Tertiary volcanism. *Bull. M.T.A.* **110**, 113–130.

Gülden, T. (1990). *Untersuchungen zur hydrothermalen alteration und an Flüssigkeitseinschlüssen im Gebiet des Sarp Dag, Provinz Canakkale, West Türken*. M.Sc. thesis (unpubl.), Univ. Claustal, 118 pp.

Heald, P., Foley, N.K. & Hayba, D.O. (1987). Comparative anatomy of volcanic-hosted epithermal deposits: acid-sulfate and adularia–sericite types. *Econ. Geol.*, **82**,1–26.

Hedenquist, J.W., Yukihiro, M., Izawa, E., White, N.C., Giggenbach W.F. & Aohi, M. (1994). Geology, geochemistry and origin of high sulfidisation Cu-Au mineralization in the Nansatsu District, Japan. *Econ. Geol.*, **89**, 1–30.

Henley, R.W. & Ellis, A.J. (1983). Geothermal systems ancient and modern: a geochemical review. *Earth Sci. Rev.*, **19**, 1–50.

Innocenti, F. & Mazzuoli, R. (1973). Petrology of the Izmir–Karaburun volcanic area (West Turkey). *Bull. Volcanologique*, **36**, 83–104.

Meyer, C. & Hemley, J.J. (1967). Wall rock alteration. *In*: Barnes, H.L. (Ed.), *Geochemistry of Hydrothermal Ore Deposits*, 1st Edn., Holt Rinehart & Winston, New York, 166–235.

Mitchell, A.H.G. (1992). Andesitic arcs, epithermal gold and porphyry-type mineralisation in the western Pacific and Eastern Europe. *Trans. Instn. Min. Metall.*, **B101**, B125–B138.

Okay, A.I., Sengör, A.M.C. & Görür, N. (1994). Kinematic history of the opening of the Black Sea and its effect on the surrounding regions. *Geology*, **22**, 267–270.

Robertson, A.H.F. & Dixon, J.E. (1985). Introduction: aspects of the geological evolution of the Eastern Mediterranean. *Spec. Publ. Geol. Soc.*, **17**, 1–74.

Sengör, A.M.C. (1992). The Palaeo-Tethyan suture: A line of demarcation between two fundamentally different architectural styles in the structure of Asia. *The Island Arc*, **1**, 78–91.

---- & Yilmaz, Y. (1981). Tethyan evolution of Turkey: a plate tectonic approach. *Tectonophysics*, **75**, 181–241.

Seyitoglu, G. & Scott, B.C. (1992). Late Cenozoic volcanic evolution of the northeastern Aegean region. *J. Volcanol. Geother. Res.*, **34**, 157–176.

Sillitoe, R.H. (1983). Enargite-bearing massive sulfide deposits high in

porphyry copper systems. *Econ. Geol.*, **78**, 348–352.

---- (1991). Gold metallogeny of Chile - An Introduction. *Econ. Geol.*, **86**, 1187–1205.

Sillitoe, R.H., Angeles, C.A., Concia, G.M., Antiqua, E.C. & Abeya, R.B. (1990). An acid-sulfate-type gold deposit at Nalesbitan, Luzon, Philippines. *J. Geochem. Expl.*, **35**, 376–412.

Yilmaz, Y. (1989). The origin of young volcanic rocks of Western Turkey. *In*: Sengör, A.M.C. (Ed.), *Tectonic Evolution of the Tethyan Region*. Kluwer Academic Publishers, The Hague, 159–189.

---- (1990). Comparison of young volcanic associations of western and eastern Anatolia formed under a compressional regime: a review. *J. Volcanol. Geother. Res.*, **44**, 69–87.

Zimmerman, J.L., Saupe, F., Ozgen, S. & Anil, M. (1989). Oligocene–Miocene K–Ar ages of the quartz–monzonite stocks from Nevruz–Cakiroba (Yenice, Canakkale, northwest Turkey). *Terra Abs.*, **1**, 354.